View metadata, citation and similar papers at core.ac.uk

brought to you by CORE

provided by Elsevier - Publisher Connector

Cell, Vol. 123, 581–592, November 18, 2005, Copyright ©2005 by Elsevier Inc. DOI 10.1016/j.cell.2005.10.023

Histone H3 Methylation by Set2 Directs Deacetylation of Coding Regions by Rpd3S to Suppress Spurious Intragenic Transcription

Michael J. Carrozza,[1] Bing Li,[1] Laurence Florens,[1] Tamaki Suganuma,[1] Selene K. Swanson,[1] Kenneth K. Lee,[1] Wei-Jong Shia,[1] Scott Anderson,[2] John Yates,[2] Michael P. Washburn,[1] and Jerry L. Workman[1,*]

[1]Stowers Institute for Medical Research
1000 East 50th Street
Kansas City, Missouri 64110

[2]The Scripps Research Institute
10550 North Torrey Pines Road
LaJolla, California 92037

Summary

Yeast Rpd3 histone deacetylase plays an important role at actively transcribed genes. We characterized two distinct Rpd3 complexes, Rpd3L and Rpd3S, by MudPIT analysis. Both complexes shared a three subunit core and Rpd3L contains unique subunits consistent with being a promoter targeted corepressor. Rco1 and Eaf3 were subunits specific to Rpd3S. Mutants of *RCO1* and *EAF3* exhibited increased acetylation in the *FLO8* and *STE11* open reading frames (ORFs) and the appearance of aberrant transcripts initiating within the body of these ORFs. Mutants in the RNA polymerase II-associated *SET2* histone methyltransferase also displayed these defects. Set2 functioned upstream of Rpd3S and the Eaf3 methyl-histone binding chromodomain was important for recruitment of Rpd3S and for deacetylation within the *STE11* ORF. These data indicate that Pol II-associated Set2 methylates H3 providing a transcriptional memory which signals for deacetylation of ORFs by Rpd3S. This erases transcription elongation-associated acetylation to suppress intragenic transcription initiation.

Introduction

The *S. cerevisiae* Rpd3 histone deacetylase regulates the transcription of a wide range of genes. Rpd3 is involved in both activation and repression of transcription. For instance, Rpd3 is necessary for repression of genes involved in meiosis and metabolism (Kadosh and Struhl, 1997; Rundlett et al., 1998; Vidal and Gaber, 1991) and for activation of genes involved in heat shock and osmotic stress (De Nadal et al., 2004).

Rpd3 is delivered to genes by at least two mechanisms. One involves direct recruitment to gene promoters through contacts with DNA binding repressor proteins. On the *INO1* promoter the sequence-specific transcription repressor Ume6 recruits Rpd3 through interaction with the Rpd3 associated corepressor protein Sin3 (Kadosh and Struhl, 1997; Rundlett et al., 1998). This recruitment generates a two nucleosome region of histone deacetylation surrounding the Ume6 binding site (Kadosh and Struhl, 1998). The second recruitment mechanism involves Rpd3 suppression of genome wide histone acetylation levels that is independent of sequence-specific repressor proteins (Kurdistani and Grunstein, 2003). *RPD3* mutants display increased acetylation levels in both intergenic and coding regions (Robyr et al., 2002; Vogelauer et al., 2000).

Rpd3 functions as part of corepressor protein complexes. There are two known Rpd3 complexes within *S. cerevisiae* that were identified primarily by their gel filtration elution profiles (Kasten et al., 1997; Lechner et al., 2000; Rundlett et al., 1996). One complex has an apparent size of 0.6 MDa and the other 1.2 MDa. Several proteins are known to associate with Rpd3. These include Sin3, Eaf3, Cti6, Pho23, Sap30, Ume1, Rxt2, Rxt3, Rco1, Eaf3, and Sds3 (Gavin et al., 2002; Ho et al., 2002; Kadosh and Struhl, 1997; Kurdistani et al., 2002; Lechner et al., 2000; Loewith et al., 2001; Puig et al., 2004; Zhang et al., 1998). However, the distribution of these proteins within the two Rpd3 complexes and their functions remain unresolved. Before this report, only Sin3 and Sds3 were known components of the 1.2 MDa complex and the composition of the smaller complex was entirely unknown.

We sought to purify and analyze the subunit composition of the two Rpd3 complexes with three goals in mind: (1) to assign the known Rpd3 interacting proteins to each respective complex, (2) to biochemically identify any remaining unknown subunits of these complexes, and (3) to gain insights into the mechanisms of recruitment and functions of Rpd3 at positions in the genome beyond specifically targeted promoters. Toward these goals we separated and purified the large Rpd3L and small Rpd3S complexes through a combination of affinity and conventional chromatography. We then systematically identified the subunits of Rpd3L and Rpd3S complexes through multidimensional protein identification technology (MudPIT) (Washburn et al., 2001; Wolters et al., 2001). Both complexes shared a core set of three subunits including Rpd3, Sin3, and Ume1. Rpd3L also contained eight subunits previously identified to associate with Rpd3 and several novel subunits. The components of Rpd3L are consistent with it being the promoter recruited co-repressor form of Rpd3 complexes. Clues from the subunit analysis of Rpd3S led to further experiments which revealed a strikingly different function for this complex. Our experiments illustrate that Rpd3S functions in a signaling pathway from elongating RNA Pol II through the Set2 histone methyltransferase. Rpd3S recognizes the Set2 methylated histones and deacetylates histones within transcribed sequences. This erases transcription elongation-associated histone acetylation and serves to repress the occurrence of spurious transcription initiation from cryptic start sites within open reading frames.

Results

Purification of the Small and Large Rpd3 Complexes

Previous studies identified two *S. cerevisiae* Rpd3 complexes that elute from gel filtration chromatography

*Correspondence: jlw@stowers-institute.org

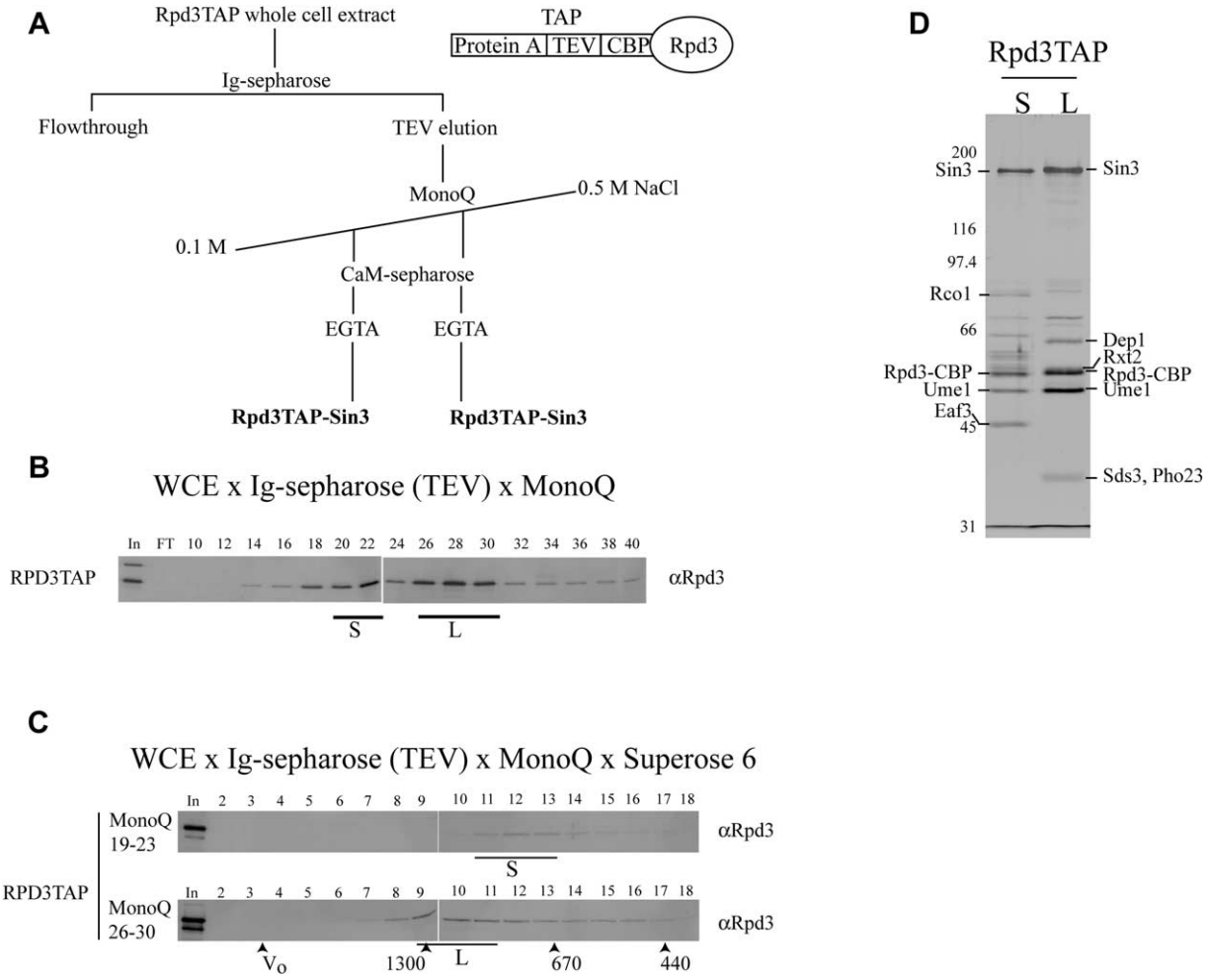

Figure 1. Purification of Rpd3-Sin3 Complexes

(A) Fractionation scheme for TAP purification of small and large Rpd3 complexes from TAP-tagged Rpd3 (YJW652) or Sin3 (YJW620) cells.
(B) MonoQ ion-exchange fractions.
(C) Superose 6 gel filtration of Rpd3 complexes. In both (B) and (C), fractions were analyzed by Western using an Rpd3 antibody. Bars below Westerns indicate peak fractions for Rpd3S (S) and Rpd3L (L).
(D) Purified small and large Rpd3 complexes. Samples were resolved on 8% SDS-gels and silver stained. Bands known to correspond to different subunits are indicated.

at apparent sizes of 0.6 and 1.2 MDa (Kasten et al., 1997; Lechner et al., 2000; Rundlett et al., 1996). To gain a complete understanding of the subunits that constitute each of these complexes, whole cell extract from a tandem affinity purification (TAP) (Puig et al., 2001) tagged Rpd3 strain was subjected to a modified TAP purification that resolves the two Rpd3 complexes on a MonoQ ion-exchange column (Figure 1A). Fractions containing Rpd3 were identified by Western blot (Figure 1B). Two peaks of Rpd3 eluted from the MonoQ column, one between fractions 19 and 23 (peak S) and the other between 26 and 30 (peak L). Superose 6 gel filtration determined the size of the Rpd3 complexes in peak S and L to be at an apparent mass of 0.8 MDa and 1.3 MDa, respectively. (Figure 1C).

Fraction pools of the MonoQ peaks S and L were subsequently purified on calmodulin (CaM)-sepharose. The composition of the calmodulin eluates was analyzed by silver-stained SDS-PAGE and by MudPIT. The silver stain demonstrated that both Rpd3 preparations are composed of a distinct mixture of proteins (Figure 1D). Based upon the MudPIT analysis described below, comparison of silver stain gels from TAP purification through other Rpd3 complex subunits and purification of Rpd3 complexes from subunit deletion strains, we determined proteins corresponding to some of the bands in Figure 1D. MudPIT analysis of these two Rpd3 preparations detected most of the proteins known to associate with Rpd3 (Table 1 and Table S1 in the Supplemental Data available with this article online) (Gavin et al., 2002; Ho et al., 2002; Kadosh and Struhl, 1997; Kurdistani et al., 2002; Lechner et al., 2000; Loewith et al., 2001; Puig et al., 2004; Zhang et al., 1998). Both preparations contained Rpd3, Sin3, Ume1, Eaf3, and Rco1. The Rpd3TAP L preparation also contained a unique set of proteins, including Pho23, Sap30, Sds3,

Table 1. Composition of the Rpd3 Complexes as Determined by MudPIT Analysis

Subunit	MW (kDa)	Rpd3TAP S	Rpd3TAP L	Sin3TAP S	Sin3TAP L	Rco1TAP	Eaf3TAP	Rxt2TAP
Rpd3	48.9	*76.0[a] (264[b])*	*85.5 (201)*	*73.4 (106)*	*72.7 (150)*	*75.8[a] (36[b])*	*84.3 (100)*	*86.6 (181)*
Sin3	175	*43.0 (556)*	*69.0 (743)*	*52.7 (422)*	*46.7 (295)*	*44.1 (166)*	*44.9 (250)*	*56.2 (464)*
Ume1	51.0	*68.0 (334)*	*83.3 (314)*	*67.6 (165)*	*66.1 (162)*	*60.4 (63)*	*55.4 (88)*	*72.6 (199)*
Pho23	37.0		**65.2 (72)**		**34.8 (42)**			**49.7 (65)**
Sap30	23.0		**57.2 (110)**		**47.3 (43)**			**52.7 (47)**
Sds3	37.6		**60.9 (111)**		**49.8 (52)**			**45.6 (43)**
Cti6	57.1		**69.2 (171)**		**46.2 (72)**			**58.1 (78)**
Rxt2	48.6		**68.4 (162)**		**62 (62)**			**58.9 (91)**
Rxt3	33.8		**58.8 (26)**		**7.8 (2)**			**38.8 (20)**
Dep1	41.8		**53.0 (98)**		**34.8 (43)**			**42.5 (61)**
Ume6	91.1	**5.0 (5)**	**20.7 (16)**					**11.0 (9)**
Ash1	65.7		**58.5 (65)**		**27.2 (27)**			**54.1 (40)**
Rco1	78.8	70.6 (393)	45.9 (52)	68.6 (245)	57.2 (73)	69.6 (129)	61.5 (158)	
Eaf3	45.2	71.6 (229)	33.9 (16)	73.8 (145)	45.1 (38)	73.8 (68)	57.9 (85)	3.2 (1)

MS data for each subunit are sorted by font type (bold, underlined, and italics) according to whether it is unique to the Rpd3L complex (bold), the Rpd3S complex (underlined), or shared between complexes (italics). See Table S1 for complete data.
[a] Sequence coverage, percentage of protein sequence represented in peptides identified by tandem mass spectrometry.
[b] Spectrum count, total spectra matching peptides detected by tandem mass spectrometry for the indicated protein.

Cti6, Rxt2, Rxt3, Dep1, Ume6, and Ash1. This analysis revealed several novel proteins, including the sequence-specific repressors Ash1 and Ume6, stably associating with the Rpd3 complexes. Although not presented here, several Hsp70 chaperone homologs (Ssa and Ssb proteins) were detected in both preparations. The entire eight member chaperone ring complex Cct1-8 was detected in the Rpd3TAP S preparation. A complete list of proteins detected in all MudPIT analyses described in this paper is available in the Supplemental Data (Table S1). In addition, CaM pulldowns with TAP tagged subunits and Western analysis for Rpd3 subunits confirmed subunits relevant to the experiments described below (Figure S1).

The MonoQ fractionation shows that Rpd3TAP S and L share a number of subunits. Comparison of the total peptides or spectral count for identified proteins between the two peaks indicates the shared subunits. Spectral count can be considered as an empirical parameter to estimate protein abundance in LC/MS/MS analyses, especially when comparing the same protein across different samples (Liu et al., 2004). The spectral counts for Sin3 between the two peaks are similar with Sin3 being detected by 556 spectra in the Rpd3TAP S peak and 743 spectra in the L peak. Ume1 and Rpd3 exhibited the same pattern. Performing the same purification depicted in Figure 1A with a *SIN3TAP* strain provided further support. Comparison of the Sin3TAP and Rpd3TAP purification in Table 1 showed a Sin3 shared component since the MudPIT analysis detected the same subunits in both purifications. Thus, it appears that Rpd3, Sin3, and Ume1 represent a shared core of subunits within Rpd3S and L.

Although the MonoQ fractionation of Rpd3 complexes clearly demonstrated the presence of two complexes with distinct subunit composition, it was possible that the first MonoQ peak S was still eluting, albeit to a lesser extent, when the MonoQ L peak began to elute. This could result in subunits specific to the small complex appearing in the analysis of the large complex in Table 1. This possibility is apparent when we compared the spectral count for proteins between the two peaks. For instance, examination of the spectral counts for the apparently shared subunits, Eaf3 and Rco1, revealed some differences between the S and L peaks for both Rpd3TAP and Sin3TAP purifications. Rco1 was detected by 393 spectra in Rpd3TAP S and 52 in Rpd3TAP L, while 229 and 16 spectra matched peptides derived from Eaf3 in the Rpd3TAP S and L samples, respectively (Table 1). We observed a similar pattern in the Sin3TAP purification. This clear difference in protein levels suggested that peptides from Rco1 and Eaf3 in the Rpd3TAP L fraction are contaminants from the Rpd3TAP S peak. Furthermore, since the remaining components, Rpd3, Sin3, and Ume1 from the Rpd3TAP and Sin3TAP S preparations appear to be shared with the L preparations based on their spectral counts, it appears that Eaf3 and Rco1 are unique subunits of Rpd3TAP and Sin3TAP S peaks.

In support of this conclusion, we performed Eaf3TAP, Rco1TAP, and Rxt2TAP purifications. These were conducted using a standard TAP purification consisting of Ig-sepharose and calmodulin-sepharose affinity purification steps omitting any additional fractionation. MudPIT analysis of Rco1TAP and Eaf3TAP purifications identified a small Rpd3 complex composed of Rco1, Eaf3, and the shared core subunits Rpd3, Sin3, and Ume1 (Table 1). The Eaf3 purification also identified the components of the NuA4 histone acetyltransferase (HAT) complex. Eaf3 is a component of NuA4. For simplicity, this data is only provided in Table S1. MudPIT analysis of Rxt2TAP purification identified the unique components of Rpd3L. These were not observed in either Rco1TAP or Eaf3TAP purifications. Similarly, the Rxt2TAP purification lacked significant levels of Eaf3 and Rco1. Thus, Eaf3 and Rco1 are specific to Rpd3S. The remainder of this report focuses on the function of Rpd3S. A separate report focuses on Rpd3L function (Carrozza et al., 2005).

Rco1 and Eaf3 Are Integral Components of the Rpd3S Complex

In order to understand the importance of Rco1 and Eaf3 in the integrity of Rpd3S, we tagged Rpd3 with TAP in

Table 2. Composition of Mutant Rpd3 Complexes as Determined by MudPIT Analysis

Locus	MW (kDa)	*wt*	*eaf3Δ*	*rco1Δ*	*eaf3chdΔ*
Rpd3	48.9	*68.1*[a] *(107*[b]*)*	*82.4 (202)*	*89.1 (281)*	*63.7 (238)*
Sin3	175	*47.4 (291)*	*62.1 (585)*	*66.7 (701)*	*55.9 (685)*
Ume1	51.0	*62.4 (168)*	*70.2 (262)*	*72.6 (301)*	*55.4 (171)*
Pho23	37.0	**37.3 (28)**	**61.2 (64)**	**51.5 (61)**	**32.4 (44)**
Sap30	23.0	**50.7 (70)**	**55.7 (65)**	**58.7 (82)**	**38.8 (67)**
Sds3	37.6	**54.4 (63)**	**68.2 (95)**	**63.0 (92)**	**54.1(72)**
Cti6	57.1	**64.4 (59)**	**62.1 (93)**	**67.0 (86)**	**53.2 (116)**
Rxt2	48.6	**51.2 (75)**	**62.3 (95)**	**57.8 (107)**	**44.4 (83)**
Rxt3	33.8	**52.4 (41)**	**62.9 (52)**	**53.1 (39)**	**53.4 (41)**
Dep1	41.8	**42.3 (47)**	**33.7 (46)**	**42.3 (68)**	**18.5 (53)**
Ume6	91.1		**23.2 (19)**	**25.8 (14)**	**3.7 (3)**
Ash1	65.7	**41.0 (36)**	**46.9 (50)**	**53.1 (54)**	**32.7 (43)**
Rco1	78.8	52.0 (88)	3.1 (3)		30.7 (47)
Eaf3	45.2	43.9 (30)			30.9 (27)

MS data for each subunit are sorted by font type (bold, underlined, and italics) according to whether it unique to the Rpd3L complex (bold), the Rpd3S complex (underlined), or shared between complexes (italics). See Table S1 for complete data.
[a] Sequence coverage, percentage of protein sequence represented in peptides identified by mass spectrometry.
[b] Spectrum count, total peptides detected by mass spectrometry for the indicated protein.

an *rco1Δ* and *eaf3Δ* strain. We purified Rpd3 complexes from these strains using the standard TAP purification. Therefore, these purifications represent a mixture of all Rpd3 complexes. Each of these preparations was analyzed by MudPIT. We observed that the absence of Eaf3 destabilized association of Rco1 with Rpd3 (Table 2). In the *rco1Δ* strain, the association of Eaf3 with Rpd3 was undetectable. Therefore, Rco1 and Eaf3 require each other for stable association with Rpd3S.

Regulation of Histone Acetylation within Coding Regions by Rpd3S and Set2

In yeast, *EAF3* loss causes increased histone acetylation within coding regions and decreased acetylation within intergenic regions, while showing no change in the absolute histone H4 acetylation level (Reid et al., 2004). Eaf3 is a component of the promoter-targeted NuA4 HAT complex (Eisen et al., 2001), the loss of which can explain decreased acetylation in intergenic regions. The finding that Eaf3 is also a component of Rpd3S may explain the increased acetylation in coding regions if Rpd3S is functioning within coding regions. Similar to HP1, *Drosophila* Polycomb and yeast Chd1, Eaf3 contains a chromodomain, which could direct this protein and Rpd3S to coding regions by binding to methylated histones (Bannister et al., 2001; Lachner et al., 2001; Pray-Grant et al., 2005). The Set2 protein associates with the phosphorylated CTD of elongating RNA Pol II and methylates histone H3K36 on transcribed genes in vivo (Krogan et al., 2003b; Li et al., 2003; Xiao et al., 2003). Furthermore, Eaf3 affects acetylation within coding regions primarily in the 3′ portions (Reid et al., 2004). These observations raised the possibility that Set2 and Rpd3S regulate acetylation within the 3′ portions of coding regions.

To address this possibility, we performed acetylated histone H4 ChIPs on extracts from strains containing null mutations in either the unique Rpd3S subunit, *RCO1*, the Rpd3L subunit *DEP1, SET2* or an *EAF3* chromodomain deletion mutant (*eaf3chdΔ*). The chromodomain deletion was generated in the genomic copy of *EAF3*. MudPIT analysis of an Rpd3 purification from an *RPD3TAP eaf3chdΔ* strain demonstrated that Rco1 and Eaf3 are associated with Rpd3 in this mutant (Table 2). Western analysis of Eaf3 immunoprecipitations (Figure S2, lanes 2 and 3, upper panel) confirmed this association. Null mutants in the Rpd3 complex core subunit *SIN3* and the Rpd3S subunit *EAF3* (Reid et al., 2004) were included in ChIPs as controls. DNA from immunoprecipitations was amplified with primers corresponding to the *INO1* promoter, the *STE11* promoter or 5′ and 3′ regions of the *FLO8*, *GLT1* and *STE11* ORFs. The Rpd3S mutants *eaf3Δ*, *rco1Δ, sin3Δ, eaf3chdΔ* and the histone methyltransferase (HMT) mutant *set2Δ* showed an increased histone H4 acetylation predominantly within a more 3′ portion of coding regions, while the Rpd3L mutant *dep1Δ* showed no significant change in acetylation across all three coding regions (Figure 2A). Thus, the Rpd3S complex, the Eaf3 chromodomain and Set2 are important for proper regulation of coding region acetylation. To simplify matters, in the remainder of this study, we performed ChIP analysis at coding regions with the 3′ ORF primer sets used here.

Since *set2Δ* displayed increased acetylation at coding regions, we tested whether histone H3K36 methylation is mediating the proper acetylation. We performed histone H4 acetylation ChIPs in extracts from a strain with an alanine substitution at histone H3K36 (*H3K36A*). This resulted in increased levels of acetylation comparable to that seen in *set2Δ* (Figure 2B). Thus, histone H3K36 methylation by Set2 is important for proper acetylation at coding regions.

Northern blots showed that the *STE11* promoter is transcriptionally active (Figures 5A and 5B). Under these circumstances, Rpd3 would not be predicted to have any repressive role at this promoter. None of our mutants showed any significant change in histone H4 acetylation (Figure 2C) at the *STE11* promoter. However, Rpd3 is recruited to the *INO1* promoter through the DNA binding repressor protein Ume6 (Kadosh and Struhl, 1997). The Rpd3L subunit *dep1Δ* and *sin3Δ* strains showed increased acetylation at the *INO1* promoter, while the *rco1Δ*, *eaf3Δ*, and *set2Δ* strains remain

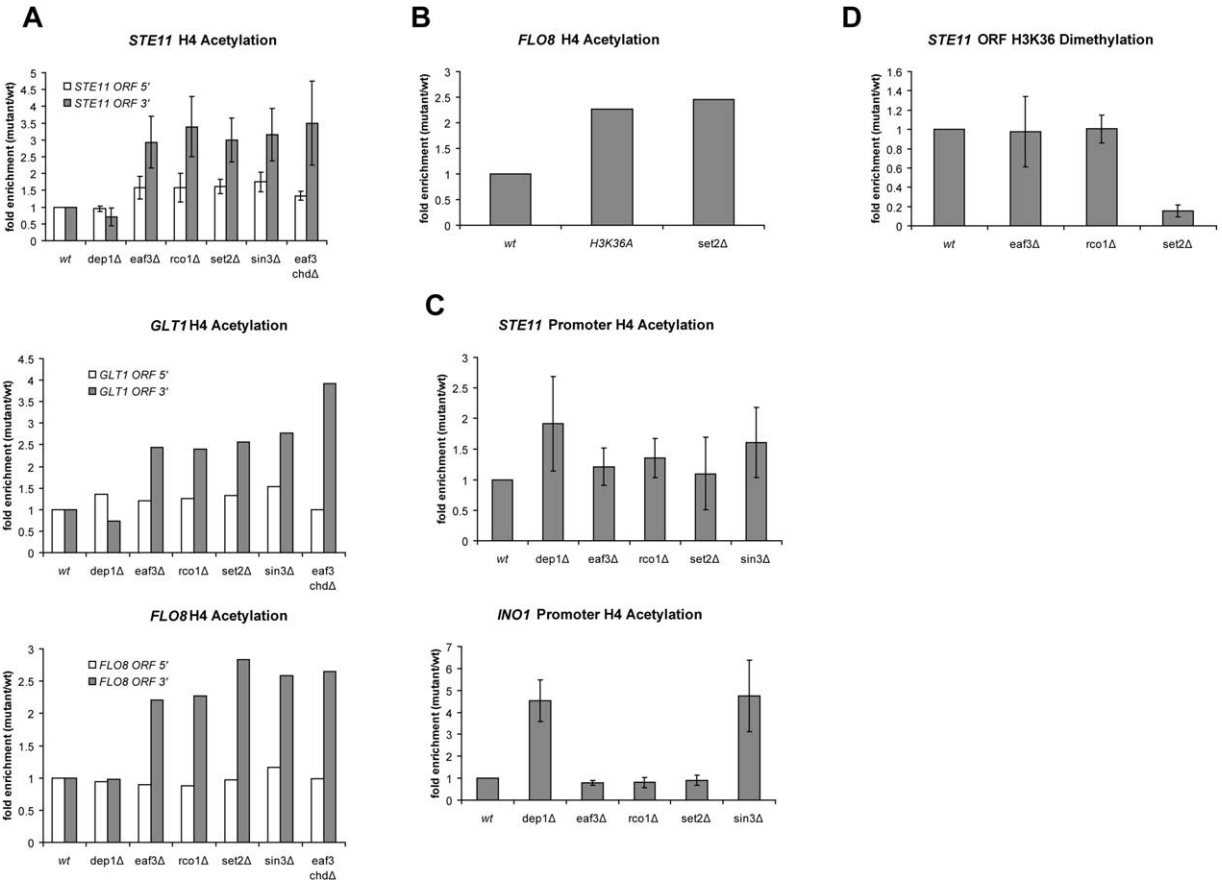

Figure 2. ChIP Analysis of Rpd3 Complex Subunits and Set2 at Coding and Promoter Regions

Crosslinked extracts from wild-type (YJW568), *dep1Δ* (YJW569), *eaf3Δ* (YJW593), *rco1Δ* (YJW646), *set2Δ* (YJW671), *sin3Δ* (YJW574), wild-type (YJW677), *eaf3chdΔ* (YJW689) wild-type (YBL574), and *H3K36A* (YBL575) strains were immunoprecipitated. Samples were amplified by PCR, run on agarose gels, and quantified. Values represent the average of two to three independent experiments. Error bars for standard deviation are provided for values representing three experiments.

(A) ChIP analysis of Rpd3S and *SET2* mutants with acetylated histone H4 antibody at the *STE11, GLT1*, and *FLO8* 5′- and 3′-coding region portions.

(B) ChIP analysis of histone H3K36 mutant with acetylated histone H4 antibody using the *FLO8* 3′ ORF primer set.

(C) ChIP analysis of Rpd3S and *SET2* mutants with acetylated histone H4 antibody at the *STE11* and *INO1* promoter region.

(D) ChIP analysis of Rpd3S and *SET2* mutants with histone H3K36me2 antibody using the *STE11* 3′ ORF primer set.

unchanged (Figure 2C). Thus, Rpd3L appears to function specifically at repressed promoters, while Rpd3S function is directed to coding regions.

We also performed ChIP for histone H3K18, which changed in patterns similar to histone H4 acetylation in different mutants (see Figure S3A). ChIP analysis using a C-terminal histone H3 antibody determined that the overall levels of histone H3 remained relatively unchanged on the *STE11* promoter, coding region and the *INO1* promoter (Figure S3B), indicating these effects are not the result of changes in histone occupancy.

We next determined the role of Rpd3S in histone H3K36 methylation. We addressed this by performing dimethylated (me2) histone H3K36 ChIPs in Rpd3S complex and *SET2* null mutants. Methylation of the *STE11* coding region was diminished in the *set2Δ* but not in *rco1Δ* and *eaf3Δ* strains (Figure 2D). The lack of an effect by Rpd3S mutants on methylation and the increased acetylation observed with the *set2Δ* strain (Figure 2A) indicates that Set2 methylation functions upstream of Rpd3S in the pathway that eventually signals for deacetylation by Rpd3.

The Eaf3 Chromodomain Directs Rpd3S to Coding Regions

We suggested above that the Eaf3 chromodomain might direct Rpd3S to coding regions methylated by Set2. To address this hypothesis, we tested *eaf3chdΔ* in ChIPs using an Eaf3 antibody. Western analysis from immunoprecipitations of wild-type and *eaf3chdΔ* determined that the Eaf3 antibody recognized the wild-type and mutant protein with equal intensity (Figure S2, lanes 2 and 3, lower panel). Enrichment of Eaf3 in the *eaf3chdΔ* strain was significantly reduced at the *STE11* ORF relative to wild-type cells (Figure 3A). Thus, binding of Eaf3 complexes to the *STE11* coding region requires the chromodomain.

We next addressed whether Eaf3 binding was depen-

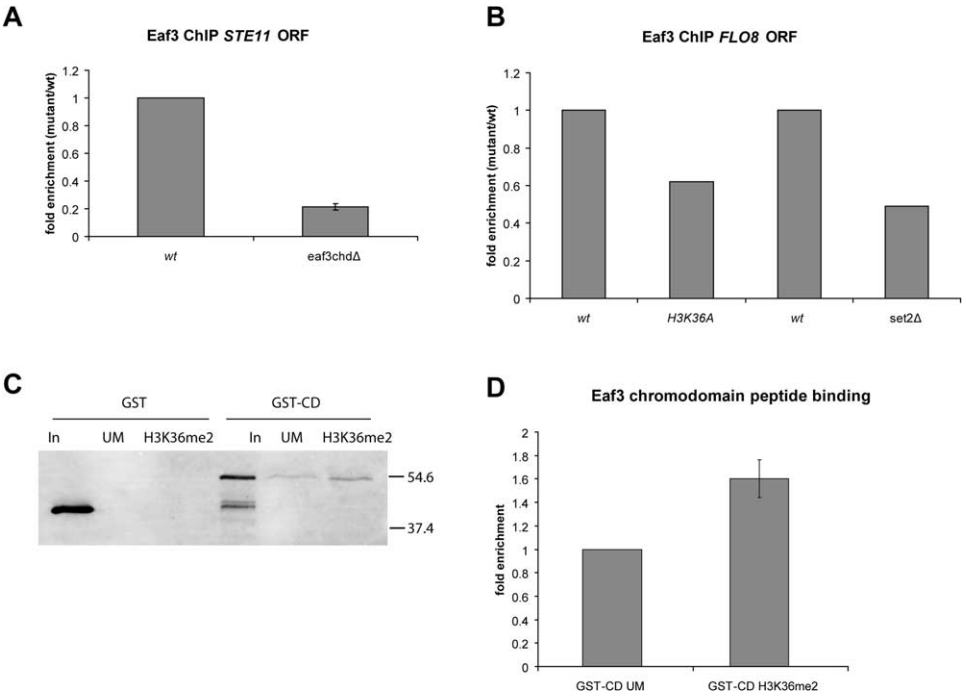

Figure 3. Eaf3 Binding to Set2 Methylated Histone H3K36

(A and B) Crosslinked extracts from wild-type (YJW677), *eaf3chd⊿* (YJW689) wild-type (YBL574), *H3K36A* (YBL575), wild-type (YJW568), and *set2⊿* (YJW671) strains were immunoprecipitated with Eaf3 antibody. PCR samples were prepared and quantified as explained in Figure 2 legend.

(A) ChIP analysis of Eaf3 binding using the *STE11* 3′ ORF primer set.

(B) Using the *FLO8* 3′ ORF primer set.

(C) Eaf3 chromodomain binding to histone H3K36 dimethylated peptide. GST or GST-Eaf3 chromodomain (GST-CD) were tested for binding to biotinylated unmodified histone H3 (UM) or histone H3K36me2 peptides immobilized on strepavidin-agarose. Input and pull-downs were run on SDS-gels and analyzed by Western blot with GST antibody.

(D) Quantification of Eaf chromodomain peptide binding. Values represent the mean (n = 4) ± standard deviation of independent experiments.

dent on Set2 and histone H3K36, by ChIP analysis of the *H3K36A* and *set2⊿* strains. Both mutations resulted in reduced Eaf3 binding at the *FLO8* coding region (Figure 3B). Thus, Eaf3 binding at coding regions is dependent on both the presence of histone H3K36 and Set2. Our observations were similar at the *STE11* and *FLO8* genes indicating that Eaf3 binding to coding regions is not a property of one particular gene.

To determine whether the Eaf3 chromodomain can directly bind methylated histone H3K36, we tested a GST-Eaf3 chromodomain for binding to a histone H3 unmodified and a K36me2 modified peptide. The chromodomain bound both peptides, relative to GST alone (Figure 3C). However, the chromodomain modestly but consistently bound the histone H3K36me2 peptide to a greater extent than the unmodified peptide (Figure 3D). It was also demonstrated that the chromodomain binds nucleosomes isolated from wild-type but not *set2⊿* cells (Keogh et al., accompanying paper). These results suggest that the chromodomain can bind directly to Set2 methylated histone H3K36.

Set2 Specifically Regulates Acetylation and Eaf3 Binding in 3′ Portions of Coding Regions

We also tested whether the other yeast HMTs Set1 and Dot1 played any role in acetylation of coding regions. Set1 and Dot1 methylate histone H3K4 and H3K79, respectively. We performed ChIP analysis using *bre2⊿*, *dot1⊿*, and *set2⊿* strains. Bre2 is a component of the Set1 containing complex COMPASS, which is required for histone H3K4 methylation (Krogan et al., 2002; Nagy et al., 2002; Roguev et al., 2001). While *set2⊿* displayed increased acetylation at the *FLO8* coding region, *bre2⊿* and *dot1⊿* showed no increase (Figure 4A). Similarly, Eaf3 binding at the *FLO8* coding region in *set2⊿* was significantly reduced, while *bre2⊿* and *dot1⊿* strains showed no reduction. Thus, proper acetylation and binding of Eaf3 is regulated specifically by the Set2 HMT.

Rpd3S and Set2 Repress Transcription Initiation from Intragenic Cryptic Promoters

HAT activities travel with RNA Pol II and facilitate elongation through downstream nucleosomes (Kristjuhan and Svejstrup, 2004; Kristjuhan et al., 2002; Wittschieben et al., 1999). An obvious function for RpdS would be to reverse histone acetylation generated during the passing of elongating RNA polymerases. Histone H3K36 methylation by the Set2 could provide a transcriptional memory of the passing polymerase and signal for Rpd3S histone deacetylation. This possibility is supported by others showing that Rpd3S (Keogh et al.,

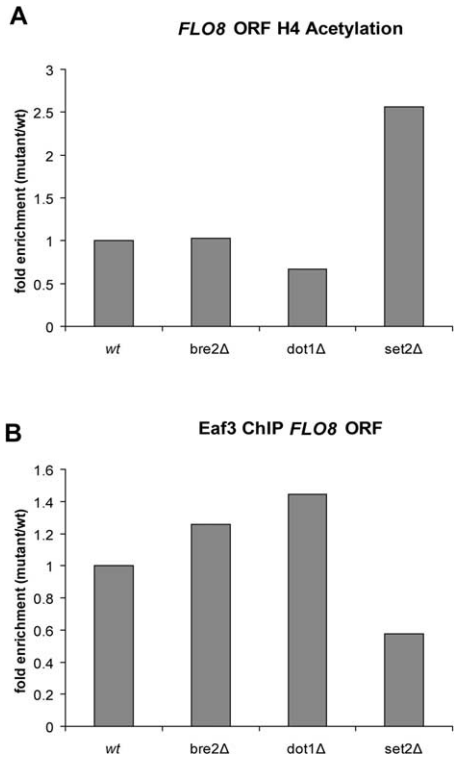

Figure 4. Regulation of Coding Region Acetylation and Eaf3 Binding by HMTs

Crosslinked extracts from wild-type (YJW568), *bre2⊿* (YJW718), *dot1⊿* (YJW719), and *set2⊿* (YJW671) strains were immunoprecipitated. PCR samples were prepared and quantified. Values represent the average of two experiments.

(A) ChIP analysis with acetylated histone H4 antibody.

(B) With Eaf3 antibody using the *FLO8* 3′ ORF primer set.

accompanying paper) and *SET2* (Kizer et al., 2005) mutants displayed an increased resistance to the drug 6-azauracil, an indication of defects in transcription elongation. Restoring the quality of chromatin behind RNA polymerases is important for the fidelity of transcription initiation. Nucleosome assembly proteins Spt6 and Spt16 act as transcription elongation factors and are required to re-establish nucleosome density on transcribed genes (Belotserkovskaya et al., 2003; Kaplan et al., 2003; Mason and Struhl, 2003; Saunders et al., 2003). In their absence, transcription initiates erroneously from cryptic promoter-like sequences within the body of several genes. Thus, stable nucleosomes of adequate density are necessary to suppress this intragenic transcription initiation and maintain the fidelity of transcription initiation. This raises the possibility that suppression of cryptic transcription requires histone deacetylation in ORFs.

SPT6 mutants display intragenic transcription initiation within the *FLO8* and *STE11* genes (Kaplan et al., 2003). Therefore, we tested for the occurrence of intragenic initiation within these genes in Rpd3S subunit mutants. Northern blot analysis demonstrated that *rco1⊿*, *eaf3⊿*, and *sin3⊿* exhibited short transcripts on *STE11* (Figure 5A, lanes 3, 4, and 6) and *eaf3chd⊿* on *STE11* and *FLO8* (Figure 5B, lane 4). However, the Rpd3L component *dep1⊿* strain maintained the full-length transcripts (Figure 5A, lane 5). As shown previously (Kaplan et al., 2003), the *spt6ts* produced short transcripts on *FLO8* and *STE11* (Figure 5B, compare lanes 13 and 14). The *spt6ts* was semipermissive under conditions tested and produced short transcripts at 30°C (Figure 5B, lane 10). The smaller *FLO8* short transcript was specific since it was absent in the cryptic TATA mutant (Figure 5B, compare lanes 10 with 12 and 14 with 16). The elongation factor *ppr2⊿* strain did not display any short transcripts (Figure 5A lane 10). Thus, Rpd3S plays a role in repressing transcription initiation from intragenic cryptic promoters.

Importantly, to establish whether Set2 methylation was responsible for suppression of intragenic transcription by Rpd3S, *set2⊿* was also tested. The *set2⊿* strain exhibited short transcripts on *STE11* and *FLO8* (Figure 5A, lane 9 and Figure 5B, lane 2). By contrast, the *shg1⊿* and *rad6⊿* strains maintained the full-length transcript of *STE11* (Figure 5A, lanes 7 and 8). Shg1 is a component of COMPASS (Krogan et al., 2002). Rad6 is involved in the histone ubiquitination that is required for methylation by Dot1 and Set1 (Briggs et al., 2002; Krogan et al., 2003a; Ng et al., 2003, 2002; Sun and Allis, 2002; Wood et al., 2003). In addition, induction of *SET1* was unable to suppress the short transcripts in a *set2⊿* strain (compare lanes 13 and 16). The histone *H3K36A* strain also exhibited short transcripts on *STE11* and *FLO8* (Figure 5B, lane 8). Based on these results, the Set2 HMT appears to play a specific role in repressing intragenic cryptic promoters.

The *STE11* short transcripts are localized to 3′ regions of the ORF (Figure 5C). Detection of these transcripts in mRNA preparations with the 3′ probe indicates that they are polyadenylated and are genuine transcripts (lane 16–19). The difference in levels and choice of short transcripts in the *spt6ts* compared to the Rpd3S and *set2⊿* mutants may reflect the more disruptive effects of the spt6ts on chromatin structure (Kaplan et al., 2003) as opposed to more subtle changes in acetylation levels in the other mutants.

Histone H3K4 trimethylation (me3) is found near the 5′ ends of transcribed genes (Ng et al., 2003). Aberrant transcription initiation within coding regions should create this modification within a 3′ transcribed region. To test this, we performed ChIPs in Rpd3S and *set2⊿* mutants with a histone H3K4me3 antibody using the *FLO8* 3′ ORF primer set. Both Rpd3S and *set2⊿* mutants resulted in increased levels of histone H3K4me3, while the Rpd3L mutant *dep1⊿* showed no significant effect (Figure 5D).

We next determined the *spt6ts* effects on acetylation and histone H3K36me2. ChIP analysis of the *spt6ts* strain exhibited increased acetylation in the *FLO8* coding region at 30°C (Figure 5E, top graph). This indicates that restoration of quality chromatin structure is important for maintaining proper acetylation within coding regions. Although there was a generalized increase in acetylation at 39°C, there was no substantial change specific to *spt6ts*. This may be the result of loss in viability due to the *spt6ts* or the loss of histone H4 as previously reported (Kaplan et al., 2003). Acetylation also increased in *spt6ts* with a *FLO8* cryptic TATA mutation,

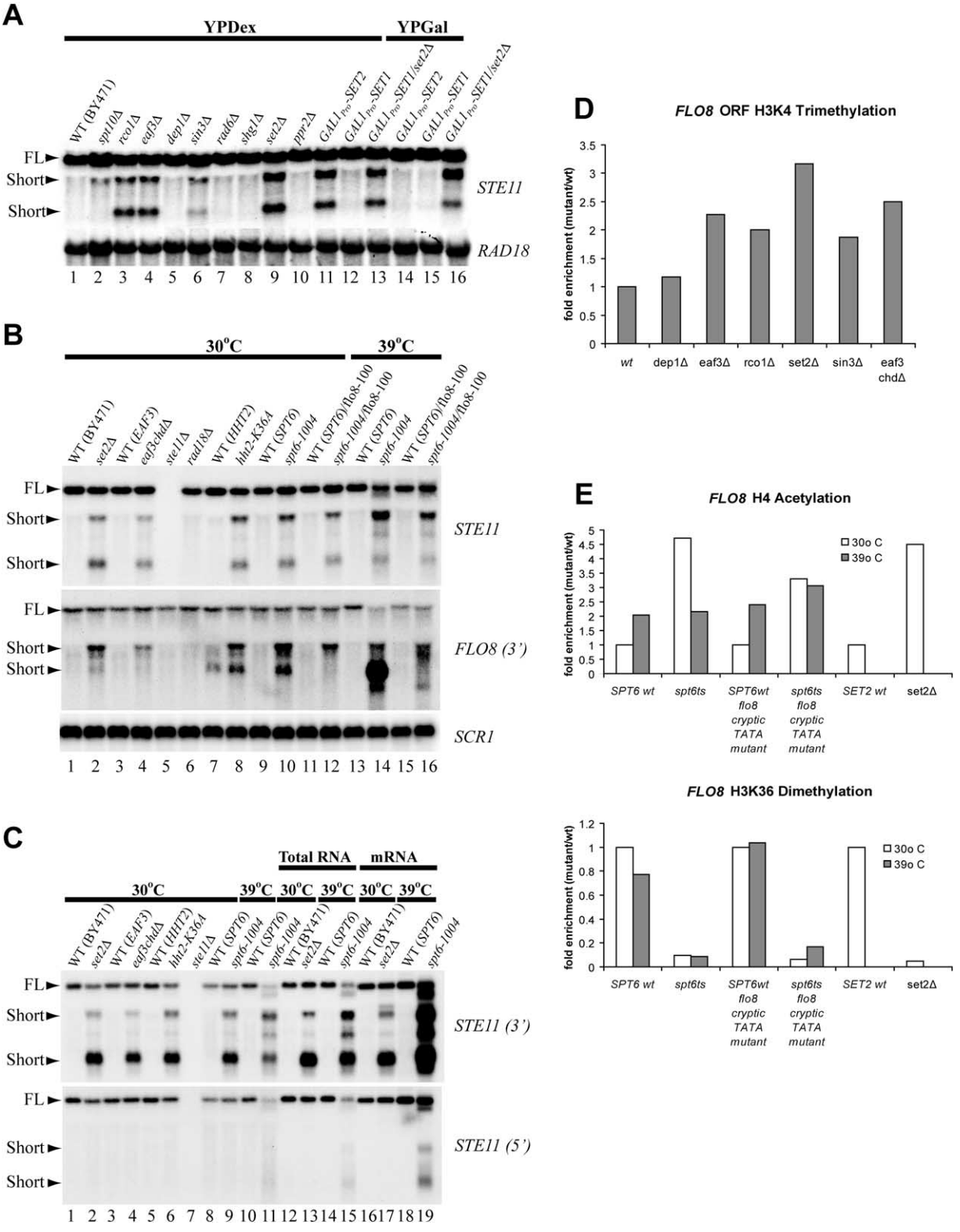

Figure 5. Rpd3S and Set2 Methylation of Histone H3K36 Repress Intragenic Spurious Transcription

(A and B) Northern blot analysis of *STE11* and *FLO8* transcripts from Rpd3 complex components and HMT mutants. RNA from wild-type (YJW568), *spt10Δ* (YBL354), *rco1Δ* (YJW594), *eaf3Δ* (YJW593), *dep1Δ* (YJW569), *sin3Δ* (YJW574), *rad6Δ* (YBL234), *shg1Δ* (YBL239), *set2Δ* (YJW671), *ppr2Δ* (CMKy80), *GAL1$_{Pro}$-SET2* (YBL287), *GAL1$_{Pro}$-SET1* (YBL288), *GAL1$_{Pro}$-SET1 set2Δ* (YBL290), wild-type (EAF3FLAG) (YJW677), *eaf3chdΔ* (YJW689), *ste11Δ* (YJW723), *rad18Δ* (YJW724), wild-type (HHT2) (YBL582), *hht2-K36A* (YBL575), wild-type (*SPT6*) (FY2181), *spt6-1004* (FY2180), wild-type (*flo8-100*) (FY2179), and *spt6-1004 flo8-100* (FY2182) strains grown in medium containing (A) dextrose

indicating that acetylation was not solely a consequence of the intragenic transcription. The *FLO8* 3′ ORF primer set amplifies a region that contains the cryptic promoter (Kaplan et al., 2003).

The *spt6ts* also exhibited a loss of histone H3K36me2 at both temperatures (Figure 5E, bottom graph), indicating that Spt6 function is also needed for Set2 methylation. Histone H3K36me2 was also disrupted in the *spt6ts* cryptic TATA mutant, indicating that this loss of methylation is not caused by the intragenic transcription.

Overall, our analysis determined that Rpd3S and Rpd3L share a core of subunits. The shared core, Rco1 and Eaf3 comprised the Rpd3S complex. Rpd3S functions in repressing intragenic transcription through histone deacetylation. This repression occurs through the Eaf3 chromodomain that recognizes the histone methylation mediated by Set2.

Discussion

Control of Coding Region Histone Acetylation through Histone Methylation

The work presented here demonstrated that methylation of histone H3K36 by Set2 directs deacetylation by Rpd3S. Interestingly, while changes in acetylation within coding regions in Rpd3S and *SET2* mutants were localized to more 3′ portions (Figure 2A), and genome wide analysis determined that while H3K36 methylation progressively increases in a 3′ direction (Pokholok et al., 2005), there is still evidence of this methylation throughout the coding region (Krogan et al., 2003b; Morillon et al., 2005; Schaft et al., 2003; Xiao et al., 2003). This suggests that additional layers exist to regulate Rpd3S activity in coding regions. The current evidence suggests that events occurring in the 5′ portion of genes influence how efficiently Rpd3 deacetylates across an ORF. Genome wide studies indicate that histone H3K4 methylation peaks at the 5′ end of transcribed genes and dissipates across the coding region (Ng et al., 2003; Pokholok et al., 2005). Perhaps, this overlap in histone H3K4 and H3K36 methylation favors acetylation in this 5′ region.

Histone H3K4 methylation stimulates acetylation through the chromodomain protein Chd1 which is found in both SLIK and the related SAGA HAT complex (Pray-Grant et al., 2005). In addition, Eaf3 as part of NuA4 may recognize histone H3K36 and H3K4 methylation in 5′ portions of the genes. Recruitment of NuA4 and histone H4K8 acetylation at the *MET16* promoter depend on Set1 and Set2 (Morillon et al., 2005). Perhaps, the combined effects of SAGA-related complexes and NuA4 overcome Rpd3S deacetylation in this part of the coding region. As histone H3K4 methylation dissipates and H3K36 methylation remains intact in more 3′ portions of the coding region, the equilibrium between HATs and HDACs may shift to favor a hypoacetylated histone pattern through the mechanism we described in this report.

Histone Acetylation within Coding Regions

The dynamics of histone exchange around the elongating polymerase remain unclear. The FACT complex and Spt6 facilitate the disassembly of nucleosomes ahead of and reassembly in the wake of the elongating polymerase (Belotserkovskaya et al., 2003). Reflective of Rpd3S, the FACT component Spt16 or Spt6 mutants also exhibit aberrant transcription initiation (Kaplan et al., 2003; Mason and Struhl, 2003). Thus, the proper reassembly by FACT, Spt6, and deacetylation by Rpd3S of nucleosomes within transcribed regions is important for repressing cryptic promoters.

What remains unclear is the extent the elongation machinery restores the nucleosome with the original and new histones. The observation that higher eukaryotes replace histone H3 with the histone H3.3 variant at actively transcribed regions indicates that histone turnover does occur during transcription (Schwartz and Ahmad, 2005). Yeast may use this mechanism but, the lack of a histone H3 variant would obstruct its identification, because histone H3.3 is the only histone H3 in yeast. The transfer of preexisting histones through the elongation machinery appears to occur as well. FACT and Spt6 bind the H2A/H2B dimer and histone H3, respectively (Belotserkovskaya et al., 2003; Bortvin and Winston, 1996). Through these interactions, FACT and Spt6 appear to serve as histone chaperones and facilitate histone passage through the elongation machinery. It is possible that FACT and Spt6 participate in the deposition of new histones.

The origins of redeposited histones may provide insight into the purpose for methylation and acetylation during elongation. Perhaps, histone acetylation facilitates histone interaction with FACT and Spt6. If the preexisting histones are redeposited, this would imply that Rpd3S removes the acetylation that occurred during their transfer through the elongation machinery. In support of this model, the RNA Pol II associated elongator complex subunit Elp3 is a HAT (Wittschieben et al., 1999). Alternatively, nucleosome assembly on transcribed DNA may involve new histones in an acetylated form. DNA replication dependent deposition of histone H3-H4 heterodimers by CAF1 requires histone acetylation by HAT1 (Verreault et al., 1996). Similarly, replica-

or galactose or (B) and (C) at 30°C and 39°C. Filters were probed with full-length sequence complementary to *STE11,* 5′ and 3′ regions of *STE11*, 3′ region of *FLO8* and as a loading control either *RAD18* or *SCR1*. The full-length (FL) and short transcript signals for *STE11* and *FLO8* are indicated. (D) ChIP analysis of H3K4me3 in Rpd3S and *set2Δ* mutants. Crosslinked extracts from wild-type (YJW568), *dep1Δ* (YJW569), *eaf3Δ* (YJW593), *rco1Δ* (YJW646), *set2Δ* (YJW671), *sin3Δ* (YJW574), wild-type (YJW677), and *eaf3chdΔ* (YJW689) were immunoprecipitated using histone H3K4me3 antibody. (E) ChIP analysis of *SPT6* and *FLO8* cryptic TATA mutants. Crosslinked extracts prepared from wild-type (*SPT6*) (FY2181), *spt6-1004* (FY2180), wild-type (*flo8-100*) (FY2179), and *spt6-1004 flo8-100* (FY2182) grown at 30°C and 39°C were immunoprecipitated using acetylated histone H4 antibody (top graph) and histone H3K36me2 antibody (bottom graph). (D and E) PCR samples were prepared and quantified. Fold enrichment was determined as the ratio of the normalized wild-type or mutant to the isogenic wild-type at 30°C. Values represent the average of two experiments.

tion independent deposition of the histone H3.3-H4 heterodimer involves the HIRA complex (Ray-Gallet et al., 2002; Tagami et al., 2004). Perhaps, HIRA also requires acetylation for its deposition function.

In either case, it is conceivable that acetylated histone deposition would create a chromatin environment amenable to transcription initiation from cryptic promoters within coding regions. The close association of Set2 with the elongating polymerase may mark through methylation the redeposited new or preexisting histones for deacetylation by Rpd3S.

Role of Rpd3S and Eaf3 in Other Organisms

We demonstrated here the importance of the Eaf3 chromodomain in repression of cryptic promoters within coding regions. To our knowledge the impact of these spurious transcripts or *EAF3* mutants on yeast remains unknown. Eaf3 is highly conserved from yeast to humans and appears to be important in higher organisms. For instance, the Eaf3 ortholog MRG15 in *Drosophila* and mice is important for proper embryonic development (Kusch et al., 2004; Tominaga et al., 2005). Another notable example is the human protein MORF4 (Bertram et al., 1999). This protein is nearly homologous to MRG15 with the exception that it lacks the chromodomain. When expressed in immortal cell lines, MORF4 induces senescence. This suggests that the chromodomain in this protein family is an important component of cell division. Both MRG15 and MORF4 associate with mSin3A complexes (Yochum and Ayer, 2002). It is quite possible that defects in yeast Eaf3 lead to similar cellular senescence through genomic instability caused by expression of these aberrant transcripts within coding regions. The effects of this improper transcription may only become apparent in older cells and go unnoticed under normal culture conditions.

Experimental Procedures

Strains and Plasmids

The strains used in this study are listed in Table S2. *RPD3TAP* (YJW652) and *RXT2TAP* (YJW670) strains in the w303 background were constructed by PCR-mediated integration using the plasmid pBS1479 as described (Puig et al., 2001). *RPD3TAP, eaf3Δ* (YJW666) was generated by PCR-mediated gene disruption of *EAF3* in YJW612. *RPD3TAP, rco1Δ* (YJW667) was created through a cross between YJW612 and YJW646. The Eaf3 chromodomain mutant (YJW689) was constructed using the modified *delitto perfetto* method (Storici et al., 2003), deleting amino acids 77-113. *RPD3TAP, eaf3chdΔ* (YJW673) was created through a cross between YJW612 and YJW689. The remaining TAP tagged and null mutant strains were purchased from Open Biosystems. The histone H3K36 mutant (YBL575) strain was made by plasmid shuffling with a wild-type histone H3 on a URA3 marker.

Tandem Affinity Purification of Protein Complexes

TAP purifications were carried out as described previously (Wu and Winston, 2002) with several modifications. Briefly, extracts from 6–12 liters of cells were incubated with Ig-sepharose and eluted with TEV protease. The eluate was incubated with calmodulin-sepharose and eluted with EGTA. For purification of Rpd3 complexes, the TEV cleavage eluate was applied to a 1 ml MonoQ anion-exchange column and eluted over a 25 ml linear 0.1– 0.5 M NaCl gradient. Gel filtration analysis was carried out using a 24 ml Superose 6 column (Amersham). Fractions were analyzed by Western using an Rpd3 antibody (Upstate Biotechnology). A more detailed description of purifications is provided in the Supplemental Data.

MudPIT Analysis of Protein Complexes

Mass spectrometry of protein complexes by MudPIT was performed as described previously (McDonald et al., 2002; Washburn et al., 2001; Wolters et al., 2001). The algorithm 2 to 3 (Sadygov et al., 2002) was used to determine charge state and to delete poor quality spectra. Matches to MS/MS spectra to peptides from a *S. cerevisiae* protein sequence database (NCBI) were determined using the program SEQUEST (Eng et al., 1994). Peptide/spectrum matches were sorted using the program DTAselect (Tabb et al., 2002). The program CONTRAST was used to compare peptides between protein complexes (Tabb et al., 2002).

Northern Analysis

Yeast Strains were grown at 30°C and 39°C in YP+ 2% dextrose or YP+ 2% galactose with 20 ug/ml of adenine. Total RNA was prepared by glass bead disruption; resolved on agarose-formaldehyde gels and transferred to Zeta-Probe membrane (Bio-RAD) (Guthrie and Fink, 1991) (Li and Reese, 2001). mRNA was purified on oligo-dT resin (Ambion). RNA was crosslinked to the membrane by UV irradiation and drying. Hybridization was carried out in 6X SSC, 5X Denhardt's solution, 0.5% SDS and 0.1 mg/ml of salmon sperm DNA. Probes (full-length, 3′ FLO8 +1672–+2399, 5′ STE11 +1–+593, and 3′ STE11 +1641–+2153) were generated by PCR.

Chromatin Immunoprecipitation Analysis

ChIPs were done as described previously (Hecht and Grunstein, 1999). Immunoprecipitations were performed using: 3 μl of anti-acetyl histone H4 (Upstate Biotechnology), 2 μl of anti-dimethyl histone H3 (Lys36) (Upstate Biotechnology), 3 μl of anti-acetyl histone H3 (Lys18) (Abcam), 2 μl of anti-trimethyl histone H3 (Lys 4), 3 μl of anti-histone H3 (Abcam), 10 μl of anti-Eaf3 (Abcam). Inputs, diluted 25 fold, and undiluted ChIP were analyzed by PCR using 25 cycles of standard PCR conditions. Reactions were resolved on 1.2% agarose gels and scanned on a Typhoon 9400 (Amersham). Primers used relative to translation start sites corresponded to –343 and –131 for the *INO1* promoter, –432 and –157 for the *STE11* promoter, +904 and +1196 for the *STE11* ORF 3′, +310F and +593 for the *STE11* ORF 5′, +1505 and +1734 for *FLO8* 3′, +261 and +493 for *FLO8* 5′, +3241 and +3490 for *GLT1* 3′, +161 and +397 for *GLT1* 5′. The *TEL* loading control primer set corresponded to a region 500 bp from the right arm of chromosome 6 (Vogelauer et al., 2000). ChIP were quantified by normalizing band intensities for each sample using the formula: (specific gene IP / *TEL* IP)/(specific gene Input / *TEL* Input). Fold enrichment was determined as the ratio of the normalized wild-type or mutant to the isogenic wild-type ChIP.

Peptide Pull-down Assay

GST or GST-Eaf3 Chromodomain (aa 67–127) (1 μg) from bacterial overexpression was incubated in binding buffer (20mM Tris-HCl [pH 8.0], 250mM NaCl, 1mM EDTA, 0.5% NP-40, 1mM PMSF, 1mM DTT, and protease inhibitor cocktail [Roche]) with 10 μg of BSA and 1 μg biotinylated dimethylated histone H3K36 peptide or histone H3 unmodified aa 22-44 (Sigma Genosys) immobilized on strepavidin-agarose. The beads were then washed with binding buffer and analyzed by Western with antibody against GST (Z-5, Santa Cruz) Western band intensities were quantified on a Typhoon 9400. Fold enrichment was expressed as the ratio of the percent input GST-CD binding on histone H3 unmodified or K36me2 peptide over the unmodified peptide.

Supplemental Data

Supplemental Data include Supplemental Experimental Procedures, three figures, two tables, and Supplemental References and can be found with this article online at http://www.cell.com/cgi/content/full/123/4/581/DC1/.

Acknowledgments

We would like to thank Nevan Krogan, Jack Greenblatt, Michael Keogh, Steve Buratowski, and Jacques Cote for sharing unpublished results; Kevin Struhl and Michael Grunstein for sharing primer sequences; Fred Winston for providing yeast strains; and Sevinc Ercan for critical reading of the manuscript. This work was supported by postdoctoral fellowship grant PF-02-012-01-GMC from the American Cancer Society to M.J.C. and NIGMS, National Institutes of Health grant GM047867 to J.L.W.

Received: May 31, 2005
Revised: September 19, 2005
Accepted: October 20, 2005
Published: November 17, 2005

References

Bannister, A.J., Zegerman, P., Partridge, J.F., Miska, E.A., Thomas, J.O., Allshire, R.C., and Kouzarides, T. (2001). Selective recognition of methylated lysine 9 on histone H3 by the HP1 chromo domain. Nature *410*, 120–124.

Belotserkovskaya, R., Oh, S., Bondarenko, V.A., Orphanides, G., Studitsky, V.M., and Reinberg, D. (2003). FACT facilitates transcription-dependent nucleosome alteration. Science *301*, 1090–1093.

Bertram, M.J., Berube, N.G., Hang-Swanson, X., Ran, Q., Leung, J.K., Bryce, S., Spurgers, K., Bick, R.J., Baldini, A., Ning, Y., et al. (1999). Identification of a gene that reverses the immortal phenotype of a subset of cells and is a member of a novel family of transcription factor-like genes. Mol. Cell. Biol. *19*, 1479–1485.

Bortvin, A., and Winston, F. (1996). Evidence that Spt6p controls chromatin structure by a direct interaction with histones. Science *272*, 1473–1476.

Briggs, S.D., Xiao, T., Sun, Z.W., Caldwell, J.A., Shabanowitz, J., Hunt, D.F., Allis, C.D., and Strahl, B.D. (2002). Gene silencing: trans-histone regulatory pathway in chromatin. Nature *418*, 498.

Carrozza, M.J., Florens, L., Swanson, S.K., Shia, W.-J., Anderson, S., Yates, J., Washburn, M.P., and Workman, J.L. (2005). Stable incorporation of sequence specific repressors Ash1 and Ume6 into the Rpd3L complex. BBA — Gene Structure and Expression. in press.

De Nadal, E., Zapater, M., Alepuz, P.M., Sumoy, L., Mas, G., and Posas, F. (2004). The MAPK Hog1 recruits Rpd3 histone deacetylase to activate osmoresponsive genes. Nature *427*, 370–374.

Eisen, A., Utley, R.T., Nourani, A., Allard, S., Schmidt, P., Lane, W.S., Lucchesi, J.C., and Cote, J. (2001). The yeast NuA4 and Drosophila MSL complexes contain homologous subunits important for transcription regulation. J. Biol. Chem. *276*, 3484–3491.

Eng, J.K., McCormack, A.L., and Yates, J.R., 3rd. (1994). An approach to correlate tandem mass spectral data of peptides with amino acid sequences in a protein database. J. Am. Soc. Mass Spectrom. *5*, 976–989.

Gavin, A.C., Bosche, M., Krause, R., Grandi, P., Marzioch, M., Bauer, A., Schultz, J., Rick, J.M., Michon, A.M., Cruciat, C.M., et al. (2002). Functional organization of the yeast proteome by systematic analysis of protein complexes. Nature *415*, 141–147.

Guthrie, C., and Fink, G.R. (1991). Guide to yeast genetics and molecular biology (San Diego: Academic Press).

Hecht, A., and Grunstein, M. (1999). Mapping DNA interaction sites of chromosomal proteins using immunoprecipitation and polymerase chain reaction. Methods Enzymol. *304*, 399–414.

Ho, Y., Gruhler, A., Heilbut, A., Bader, G.D., Moore, L., Adams, S.L., Millar, A., Taylor, P., Bennett, K., Boutilier, K., et al. (2002). Systematic identification of protein complexes in Saccharomyces cerevisiae by mass spectrometry. Nature *415*, 180–183.

Kadosh, D., and Struhl, K. (1997). Repression by Ume6 involves recruitment of a complex containing Sin3 corepressor and Rpd3 histone deacetylase to target promoters. Cell *89*, 365–371.

Kadosh, D., and Struhl, K. (1998). Targeted recruitment of the Sin3-Rpd3 histone deacetylase complex generates a highly localized domain of repressed chromatin in vivo. Mol. Cell. Biol. *18*, 5121–5127.

Kaplan, C.D., Laprade, L., and Winston, F. (2003). Transcription elongation factors repress transcription initiation from cryptic sites. Science *301*, 1096–1099.

Kasten, M.M., Dorland, S., and Stillman, D.J. (1997). A large protein complex containing the yeast Sin3p and Rpd3p transcriptional regulators. Mol. Cell. Biol. *17*, 4852–4858.

Kizer, K.O., Phatnani, H.P., Shibata, Y., Hall, H., Greenleaf, A.L., and Strahl, B.D. (2005). A novel domain in Set2 mediates RNA polymerase II interaction and couples histone H3 K36 methylation with transcript elongation. Mol. Cell. Biol. *25*, 3305–3316.

Kristjuhan, A., and Svejstrup, J.Q. (2004). Evidence for distinct mechanisms facilitating transcript elongation through chromatin in vivo. EMBO J. *23*, 4243–4252.

Kristjuhan, A., Walker, J., Suka, N., Grunstein, M., Roberts, D., Cairns, B.R., and Svejstrup, J.Q. (2002). Transcriptional inhibition of genes with severe histone h3 hypoacetylation in the coding region. Mol. Cell *10*, 925–933.

Krogan, N.J., Dover, J., Khorrami, S., Greenblatt, J.F., Schneider, J., Johnston, M., and Shilatifard, A. (2002). COMPASS, a histone H3 (Lysine 4) methyltransferase required for telomeric silencing of gene expression. J. Biol. Chem. *277*, 10753–10755.

Krogan, N.J., Dover, J., Wood, A., Schneider, J., Heidt, J., Boateng, M.A., Dean, K., Ryan, O.W., Golshani, A., Johnston, M., et al. (2003a). The Paf1 complex is required for histone H3 methylation by COMPASS and Dot1p: linking transcriptional elongation to histone methylation. Mol. Cell *11*, 721–729.

Krogan, N.J., Kim, M., Tong, A., Golshani, A., Cagney, G., Canadien, V., Richards, D.P., Beattie, B.K., Emili, A., Boone, C., et al. (2003b). Methylation of histone H3 by Set2 in Saccharomyces cerevisiae is linked to transcriptional elongation by RNA polymerase II. Mol. Cell. Biol. *23*, 4207–4218.

Kurdistani, S.K., and Grunstein, M. (2003). Histone acetylation and deacetylation in yeast. Nat. Rev. Mol. Cell Biol. *4*, 276–284.

Kurdistani, S.K., Robyr, D., Tavazoie, S., and Grunstein, M. (2002). Genome-wide binding map of the histone deacetylase Rpd3 in yeast. Nat. Genet. *31*, 248–254.

Kusch, T., Florens, L., Macdonald, W.H., Swanson, S.K., Glaser, R.L., Yates, J.R., 3rd, Abmayr, S.M., Washburn, M.P., and Workman, J.L. (2004). Acetylation by Tip60 is required for selective histone variant exchange at DNA lesions. Science *306*, 2084–2087.

Lachner, M., O'Carroll, D., Rea, S., Mechtler, K., and Jenuwein, T. (2001). Methylation of histone H3 lysine 9 creates a binding site for HP1 proteins. Nature *410*, 116–120.

Lechner, T., Carrozza, M.J., Yu, Y., Grant, P.A., Eberharter, A., Vannier, D., Brosch, G., Stillman, D.J., Shore, D., and Workman, J.L. (2000). Sds3 (suppressor of defective silencing 3) is an integral component of the yeast Sin3[middle dot]Rpd3 histone deacetylase complex and is required for histone deacetylase activity. J. Biol. Chem. *275*, 40961–40966.

Li, B., Howe, L., Anderson, S., Yates, J.R., 3rd, and Workman, J.L. (2003). The Set2 histone methyltransferase functions through the phosphorylated carboxyl-terminal domain of RNA polymerase II. J. Biol. Chem. *278*, 8897–8903.

Li, B., and Reese, J.C. (2001). Ssn6-Tup1 regulates RNR3 by positioning nucleosomes and affecting the chromatin structure at the upstream repression sequence. J. Biol. Chem. *276*, 33788–33797.

Liu, H., Sadygov, R.G., and Yates, J.R., 3rd. (2004). A model for random sampling and estimation of relative protein abundance in shotgun proteomics. Anal. Chem. *76*, 4193–4201.

Loewith, R., Smith, J.S., Meijer, M., Williams, T.J., Bachman, N., Boeke, J.D., and Young, D. (2001). Pho23 is associated with the Rpd3 histone deacetylase and is required for its normal function in regulation of gene expression and silencing in Saccharomyces cerevisiae. J. Biol. Chem. *276*, 24068–24074.

Mason, P.B., and Struhl, K. (2003). The FACT complex travels with elongating RNA polymerase II and is important for the fidelity of transcriptional initiation in vivo. Mol. Cell. Biol. *23*, 8323–8333.

McDonald, W.H., Ohi, R., Miyamoto, D.T., Mitchison, T.J., and Yates, J.R. (2002). Comparison of three directly coupled HPLC MS/MS strategies for identification of proteins from complex mixtures: single-dimension LCMS/MS, 2-phase MudPIT, and 3-phase MudPIT. Int. J. Mass Spectrom. *219*, 245–251.

Morillon, A., Karabetsou, N., Nair, A., and Mellor, J. (2005). Dynamic lysine methylation on histone H3 defines the regulatory phase of gene transcription. Mol. Cell *18*, 723–734.

Nagy, P.L., Griesenbeck, J., Kornberg, R.D., and Cleary, M.L. (2002). A trithorax-group complex purified from Saccharomyces cerevisiae is required for methylation of histone H3. Proc. Natl. Acad. Sci. USA *99*, 90–94.

Ng, H.H., Robert, F., Young, R.A., and Struhl, K. (2003). Targeted recruitment of Set1 histone methylase by elongating Pol II provides a localized mark and memory of recent transcriptional activity. Mol. Cell *11*, 709–719.

Ng, H.H., Xu, R.M., Zhang, Y., and Struhl, K. (2002). Ubiquitination of histone H2B by Rad6 is required for efficient Dot1-mediated methylation of histone H3 lysine 79. J. Biol. Chem. *277*, 34655–34657.

Pokholok, D.K., Harbison, C.T., Levine, S., Cole, M., Hannett, N.M., Lee, T.I., Bell, G.W., Walker, K., Rolfe, P.A., Herbolsheimer, E., et al. (2005). Genome-wide map of nucleosome acetylation and methylation in yeast. Cell *122*, 517–527.

Pray-Grant, M.G., Daniel, J.A., Schieltz, D., Yates, J.R., 3rd, and Grant, P.A. (2005). Chd1 chromodomain links histone H3 methylation with SAGA- and SLIK-dependent acetylation. Nature *433*, 434–438.

Puig, O., Caspary, F., Rigaut, G., Rutz, B., Bouveret, E., Bragado-Nilsson, E., Wilm, M., and Seraphin, B. (2001). The tandem affinity purification (TAP) method: a general procedure of protein complex purification. Methods *24*, 218–229.

Puig, S., Lau, M., and Thiele, D.J. (2004). Cti6 is an Rpd3-Sin3 histone deacetylase-associated protein required for growth under iron-limiting conditions in Saccharomyces cerevisiae. J. Biol. Chem. *279*, 30298–30306.

Ray-Gallet, D., Quivy, J.P., Scamps, C., Martini, E.M., Lipinski, M., and Almouzni, G. (2002). HIRA is critical for a nucleosome assembly pathway independent of DNA synthesis. Mol. Cell *9*, 1091–1100.

Reid, J.L., Moqtaderi, Z., and Struhl, K. (2004). Eaf3 regulates the global pattern of histone acetylation in Saccharomyces cerevisiae. Mol. Cell. Biol. *24*, 757–764.

Robyr, D., Suka, Y., Xenarios, I., Kurdistani, S.K., Wang, A., Suka, N., and Grunstein, M. (2002). Microarray deacetylation maps determine genome-wide functions for yeast histone deacetylases. Cell *109*, 437–446.

Roguev, A., Schaft, D., Shevchenko, A., Pijnappel, W.W., Wilm, M., Aasland, R., and Stewart, A.F. (2001). The Saccharomyces cerevisiae Set1 complex includes an Ash2 homologue and methylates histone 3 lysine 4. EMBO J. *20*, 7137–7148.

Rundlett, S.E., Carmen, A.A., Kobayashi, R., Bavykin, S., Turner, B.M., and Grunstein, M. (1996). HDA1 and RPD3 are members of distinct yeast histone deacetylase complexes that regulate silencing and transcription. Proc. Natl. Acad. Sci. USA *93*, 14503–14508.

Rundlett, S.E., Carmen, A.A., Suka, N., Turner, B.M., and Grunstein, M. (1998). Transcriptional repression by UME6 involves deacetylation of lysine 5 of histone H4 by RPD3. Nature *392*, 831–835.

Sadygov, R.G., Eng, J., Durr, E., Saraf, A., McDonald, H., MacCoss, M.J., and Yates, J.R., 3rd. (2002). Code developments to improve the efficiency of automated MS/MS spectra interpretation. J. Proteome Res. *1*, 211–215.

Saunders, A., Werner, J., Andrulis, E.D., Nakayama, T., Hirose, S., Reinberg, D., and Lis, J.T. (2003). Tracking FACT and the RNA polymerase II elongation complex through chromatin in vivo. Science *301*, 1094–1096.

Schaft, D., Roguev, A., Kotovic, K.M., Shevchenko, A., Sarov, M., Neugebauer, K.M., and Stewart, A.F. (2003). The histone 3 lysine 36 methyltransferase, SET2, is involved in transcriptional elongation. Nucleic Acids Res. *31*, 2475–2482.

Schwartz, B.E., and Ahmad, K. (2005). Transcriptional activation triggers deposition and removal of the histone variant H3.3. Genes Dev. *19*, 804–814.

Storici, F., Durham, C.L., Gordenin, D.A., and Resnick, M.A. (2003). Chromosomal site-specific double-strand breaks are efficiently targeted for repair by oligonucleotides in yeast. Proc. Natl. Acad. Sci. USA *100*, 14994–14999.

Sun, Z.W., and Allis, C.D. (2002). Ubiquitination of histone H2B regulates H3 methylation and gene silencing in yeast. Nature *418*, 104–108.

Tabb, D.L., McDonald, W.H., and Yates, J.R., 3rd. (2002). DTASelect and Contrast: tools for assembling and comparing protein identifications from shotgun proteomics. J. Proteome Res. *1*, 21–26.

Tagami, H., Ray-Gallet, D., Almouzni, G., and Nakatani, Y. (2004). Histone H3.1 and H3.3 complexes mediate nucleosome assembly pathways dependent or independent of DNA synthesis. Cell *116*, 51–61.

Tominaga, K., Kirtane, B., Jackson, J.G., Ikeno, Y., Ikeda, T., Hawks, C., Smith, J.R., Matzuk, M.M., and Pereira-Smith, O.M. (2005). MRG15 regulates embryonic development and cell proliferation. Mol. Cell. Biol. *25*, 2924–2937.

Verreault, A., Kaufman, P.D., Kobayashi, R., and Stillman, B. (1996). Nucleosome assembly by a complex of CAF-1 and acetylated histones H3/H4. Cell *87*, 95–104.

Vidal, M., and Gaber, R.F. (1991). RPD3 encodes a second factor required to achieve maximum positive and negative transcriptional states in Saccharomyces cerevisiae. Mol. Cell. Biol. *11*, 6317–6327.

Vogelauer, M., Wu, J., Suka, N., and Grunstein, M. (2000). Global histone acetylation and deacetylation in yeast. Nature *408*, 495–498.

Washburn, M.P., Wolters, D., and Yates, J.R., 3rd. (2001). Large-scale analysis of the yeast proteome by multidimensional protein identification technology. Nat. Biotechnol. *19*, 242–247.

Wittschieben, B.O., Otero, G., de Bizemont, T., Fellows, J., Erdjument-Bromage, H., Ohba, R., Li, Y., Allis, C.D., Tempst, P., and Svejstrup, J.Q. (1999). A novel histone acetyltransferase is an integral subunit of elongating RNA polymerase II holoenzyme. Mol. Cell *4*, 123–128.

Wolters, D.A., Washburn, M.P., and Yates, J.R., 3rd. (2001). An automated multidimensional protein identification technology for shotgun proteomics. Anal. Chem. *73*, 5683–5690.

Wood, A., Schneider, J., Dover, J., Johnston, M., and Shilatifard, A. (2003). The Paf1 complex is essential for histone monoubiquitination by the Rad6-Bre1 complex, which signals for histone methylation by COMPASS and Dot1p. J. Biol. Chem. *278*, 34739–34742.

Wu, P.Y., and Winston, F. (2002). Analysis of Spt7 function in the Saccharomyces cerevisiae SAGA coactivator complex. Mol. Cell. Biol. *22*, 5367–5379.

Xiao, T., Hall, H., Kizer, K.O., Shibata, Y., Hall, M.C., Borchers, C.H., and Strahl, B.D. (2003). Phosphorylation of RNA polymerase II CTD regulates H3 methylation in yeast. Genes Dev. *17*, 654–663.

Yochum, G.S., and Ayer, D.E. (2002). Role for the mortality factors MORF4, MRGX, and MRG15 in transcriptional repression via associations with Pf1, mSin3A, and Transducin-Like Enhancer of Split. Mol. Cell. Biol. *22*, 7868–7876.

Zhang, Y., Sun, Z.W., Iratni, R., Erdjument-Bromage, H., Tempst, P., Hampsey, M., and Reinberg, D. (1998). SAP30, a novel protein conserved between human and yeast, is a component of a histone deacetylase complex. Mol. Cell *1*, 1021–1031.